DESIGN OF COMPOSITE STRUCTURES FOR IMPROVED AEROELASTIC PERFORMANCE

G.A Vio[*,†] , I.R. Fitzpatrick[*,‡]
[*]**School of Aerospace, Mechanical and Mechatronic Engineering, The University of Sydney, Sydney NSW 2006, Australia**
[†]**gareth.vio@sydney.edu.au; [‡]ifitzpatrick@sydmey.edu.au**

Keywords: *Aeroelasticity, Flutter, Gust Response, Tailoring, Composite Design)*

Abstract

Despite the benefits of composite structures, it is only recently that the main load bearing structures in large aircraft such as the Boeing 787 and Airbus A350 have started to be manufactured using carbon fibre composites. Even then, the unique directionality properties of composite laminates and design possibilities have yet to be exploited to improve the aircraft performance. In this study a typical composite commercial aircraft wing structure is optimised using evolutionary algorithms with the aim of improving the aeroelastic response, concentrating on gust loads. Conclusions are drawn based on the performance gains that can be achieved using aeroelastic tailoring and new design idea whilst taking into account flutter and divergence constraints.

1 Introduction

In general, most traditional aircraft designs have tended to consider aeroelastic effects as troublesome annoyances, and designers have mostly dealt with through increasing the structural stiffness. This is usually accomplished with extra material and accepting the inevitable weight penalty. Whilst this has been a justifiable methodology in the past, advances in computational power and structural materials have meant that there is very little reason to not attempt to exploit these aeroelastic effects through structural tailoring for a beneficial result. The concept of aeroelastic tailoring is not a new one. A similar concept was used as early as the late 1940s by Munk [1] to design variable pitch propellers. He utilised wood ply laid up in specific orientations so as to utilise the anisotropic properties of the material to twist the blade favourably as the thrust changed. Although not specifically tailoring, Ashley et al. [2] have gathered numerous designs that account for the existence of aeroelastic effects and are designed together use the effects to their advantage or minimise their effect on the aircraft. Most of these early tailoring methods utilised changes in geometrical shape and layout in order to achieve benefits. This method of tailoring often led to trade-offs with other important design criteria, and in many cases, the aeroelastic benefits were outweighed by the detrimental effects on other areas of the design. Their rare implementation was usually due to other benefits that came in association with the changes. The idea of using the directional property of composite for aeroelastic tailoring has been around since the 70s [3]. However, since tailoring was demonstrated on the X-29 in the late 70s and early 80s, very few aircraft have used these directional properties to achieve beneficial aeroelastic effects. The original application was to reduce the likelihood of divergence occurring on forward-swept wings [3]; recent applications have included and weight reduction [4, 5, 6] and drag reduction [7] of composite wings. Although the new generation of commercial civil aircraft have started to use composites, they have only exploited the supe-

rior strength/weight ratio of composite materials rather than employ aeroelastic tailoring. As with any new technology, designing with a new material brings new challenges and possibilities. Composite manufacturing does not have the same constraints as its metal equivalent, and the possibilities that this presents will be exploited here. There are a wide range of different optimisation approaches that can be used for aeroelastic problems. Genetic algorithms have been proven to be effective for large parameter space solutions. They have been widely used as optimisation tools for a variety of problems, from plant processing system [8] to nonlinear system identification [9]. In the aeroelastic tailoring environment, genetic algorithms have been used to minimise the structural weight whilst satisfying a number of aeroelastic parameters such as flutter and divergence [4, 5, 6, 10].

Gust loads are one of the critical load cases for commercial aircraft and have a varied effect on the structures, ranging from ride roughness up to total failure of the aircraft [11]. The ability of an aircraft to withstand gust loads is one of the critical airworthiness requirements for certification but fatigue loading effects must also be considered. Gust alleviation research has concentrated in designing control systems to make use of control surface to alleviate the induced loading [12, 13, 14]. LIDAR systems have been proposed to increase the effectiveness of the control laws [15]. Gust alleviation systems in composite structures have concentrated in controlling the gust-induced vibration by embedding piezo-composite materials inside the composite lay-up [16, 17].

2 Aeroelastic Model

2.1 Structural Model

The wing model was a simple high-aspect ratio rectangular plan-form wing, with a 40 ft semi-span, 12 ft chord, and 8% thickness. The structural model approximated a typical wing-box in this configuration with skin panels top and bottom, a front and rear spar at approximately the
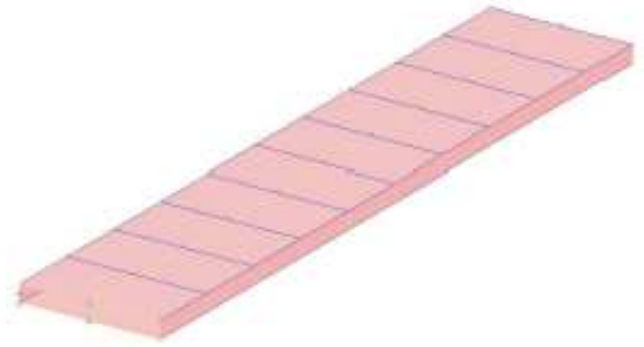
Fig. 1 Structural FE model with skin

Fig. 2 Structural FE model without skin

quarter chord and three-quarter chord points, and 10 ribs spaced evenly along the span. The root of the wing was fixed in all degrees of freedom. The thickness of the wing-box was also made constant along the chord, to aid in model creation.

The skin, spar webs and rib webs were represented by FE shell elements, and one-dimensional rod elements were used to model spar caps, rib/skin connections and rib/spar shear cleats. Non-structural mass in the wing was represented by evenly distributed concentrated mass elements at the spar/rib connection points. The structural FE model can be seen in figure 1 and 2.

The model consists of several different element types and consequently have different material choices. The shell elements used in the model were constructed from composite Graphite/Epoxy with properties listed in table 1.

E_1 (psi)	E_2 (psi)	G_{12} (psi)
18.5×10^6	1.6×10^6	0.65×10^6
ν	ρ (lb/in^3)	t (in)
0.25	0.055	0.00525

Table 1 Carbon-Epoxy Composite Material Properties

| E (psi)	G (psi)	ρ (lb/in^3)	ν
14.97×10^6	5.62×10^6	0.098	0.33

Table 2 Aluminium Material Properties

The skins were constructed of this composite Graphite/Epoxy with a symmetrical 8-ply lay-up with a layer thickness of 0.0006 *in* and fibre orientation $\begin{bmatrix} 0 & 15 & 15 & 90 \end{bmatrix}_{SYM}$ with the 0 degree fibre direction initially along the aircraft longitudinal axis (chord-wise direction). The rib and spar webs were also a symmetrical 8-ply lay-up, but this lay-up had the fibre orientation $\begin{bmatrix} 0 & +45 & 45 & 90 \end{bmatrix}_{SYM}$ giving a more even directional stiffness than the skin laminate. Finally, the spar caps, rib/skin connectors and rib/spar shear cleat elements were constructed of Aluminium, with material properties listed in table 2. The spar caps had cross-sectional areas of $[0.25, 0.2, 0.15, 0.1]$ in^2 for the front top, front bottom, rear top and rear bottom spar caps respectively. The rib connections/shear cleats had cross-sectional areas of 0.07 in^2.

Although this study is focused on composite tailoring, the actual material properties are not varied for the structural elements as part of the optimisation process, excluding the skin. This is because the objective is to optimise the overall structural shape and layout, rather than a given layout with composite materials applied.

2.2 Aerodynamic Model

The aerodynamic model consisted of a 12 *ft* chord by 40 *ft* doublet-lattice mesh which overlaps the structural wing-box model by 1 *ft* at the front spar and 3 *ft* at the rear spar, taking into account the leading and trailing edges of the wing. The mesh is 20 span-wise boxes by 12 chordwise boxes, which were chosen to satisfy
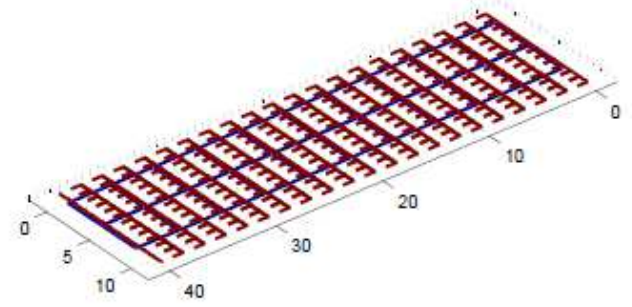
Fig. 3 Aerodynamic mesh superimposed on structural elements

the equation $\Delta x < 0.08V/f$ where Δx is the size of the chordwise division, V is the minimum velocity and f, in hertz, is the maximum frequency to be analysed. This criterion is required for accurate aerodynamic analysis. The aerodynamic loads are transferred to the structural model by spline interpolation and the mesh is set to be symmetric about the aircraft centreline (fixed end of the structural model). The doublet-lattice mesh can be seen in figure 3 overlaid on the structural model.

2.3 Aeroelastic Analysis

The aeroelastic analysis of the wing involved flutter analysis and gust impact. The flutter analysis was performed over a range of airspeeds, from 100 ft/s to 800 ft/s, and the first 8 modes of vibration were analysed, which incorporate the bending, torsion and bending-torsion coupled modes seen in classic binary flutter. The gust analysis used a '1-cosine' vertical gust profile which is used to test gust impact during certification of all aircraft [18]. The profile can be seen in figure 4. This profile has a ratio of 0.0875 for the vertical gust velocity to forward airspeed, and was tested at approximately 80% of the flutter speed for the baseline model.

3 Genetic Algorithm

Genetic Algorithms (GA) are based on the 'survival of the fittest' Darwinian theory of evolution. GAs test different solutions and the best of them
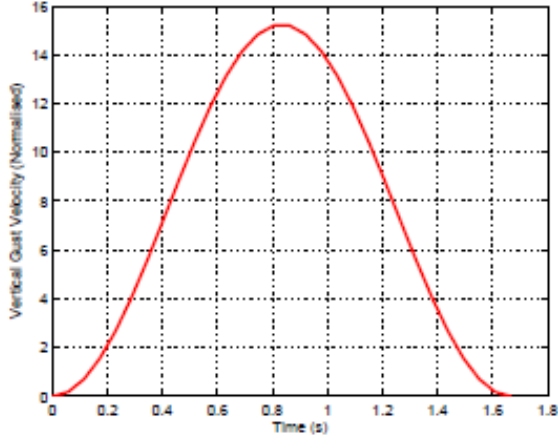
Fig. 4 '1-cosine' gust profile

are carried forward to the next iteration and are used to create new solution genes to test at the next generation. In this study the Binary implementation of the Genetic Algorithm will be used.

3.1 Binary Genetic Algorithm

The genes have a binary representation, although real number GAs have been created. The creation of new solutions is based on the following principles:

- **Crossover**. A section of a pair of genes is swapped
  0 1 1 0 | 1 0 0 0   0 1 1 0 | 0 1 0 0
  0 0 1 1 | 0 1 0 0 ⟹ 0 0 1 1 | 1 0 0 0

- **Mutation**. The value of a cell within a gene is randomly swapped
  1 0 ⓪ 1 0 0 0 0 ⟹ 1 0 ① 1 0 0 0 0

- **Translation**. The order within the gene is randomly swapped
  1 0 0 1 0 0 | 0 0 ⟹ 0 0 | 1 0 0 1 0 0

The length of each gene is dictated by the expected range of values of the solution, and has to take into account decimal places. The length of each gene is then determined by converting to binary the range times the number of decimal places required. If negative numbers are required an extra term is added to the length of the binary

Run	W_F	W_M	W_G
1	0.9	0.1	0.0
2	0.675	0.1	0.225
3	0.45	0.1	0.45
4	0.225	0.1	0.675
5	0.0	0.1	0.9

Table 3 Selection Criteria Biases in Optimisation Runs

number and when this latter is transformed to a real number, it is shifted by the value of the range.

3.2 Implementation

The selection criteria for processing genes in the BGA were derived from the modelŠs flutter velocity (F), gust response (G), and weight (M). These values were then used to calculate a cost for the gene based on the following cost function:

$$J = W_F \frac{F_1}{F_i} + W_M \frac{M_i}{M_1} + W_G \frac{G_i}{G_1} \qquad (1)$$

where W is the bias for each optimisation term with $\sum W_i = 1$, $(F/M/G)_i$ is the current value of a particular gene and $(F/M/G)_1$ is the target value.

A number of different optimisation runs were performed with different bias level in order to develop a basic Pareto frontier. Given a set of choices and a way of valuing them, the Pareto frontier is the set of choices that are Pareto efficient. A system that can make any single value (i.e. selection criteria) better without making any other any worse is not considered Pareto efficient. Thus, the Pareto frontier defines all possibilities in the system that cannot make an improvement in one criterion without making any other criteria worse. By restricting optimisation attention to the set of choices that exist on the frontier, tradeoff can be made within this set rather than considering the full range of every parameter, allowing for faster and more efficient optimisation. The selection criteria bias values for the 5 runs are listed in table 3.

3.3 Optimisation Strategy

For the optimisation, the structural model is represented by a gene string describing the optimisation parameters and their binary values. Previous studies have used laminate ply orientation, thickness, and material (fibre and matrix combinations) among other variables as parameters for optimisation studies. Whilst this study is concerned with composite materials, the majority of the optimisation parameters used focused on altering structural layouts. Due to considerable number of structural members in the model, including other variables such as those listed above increases the length of gene required to describe it (and hence size of the search space) is beyond what is acceptable for a preliminary design tool. As such the optimisation parameters used were limited to the following:

- **Skin** The top and bottom skin sections of the models were optimised for best overall fibre orientation, choosing between four options, namely; $\begin{bmatrix} 0 & 45 & 45 & 90 \end{bmatrix}$ from the freestream. Each skin section (a continuous group of shell elements) had its fibre orientation represented by 2 cells in the gene string.

- **Spars** Each spar was divided into individual sections between each rib. The spar section (shell element web and top and bottom 1D rod element caps combined) could either exist or not exist. Each section was represented by a single cell in the gene string.

- **Ribs** Each rib element ran the full length of the structural model chord, from the front spar to rear spar. These rib elements (including the rib/skin connections and rib/spar shear cleats) were again represented by a single cell which determined if it existed or not.

- **Connection Points Position** Each point where a spar or rib element connected with another spar or rib element in the initial model was classified as a connection point. Connection points were given the ability to move from their initial positions by a predetermined value and in a given direction. These directions were forward, backward, left or right ($\pm X, \pm Y$) when looking down on the model from above (XY Plane). A single cell (Boolean) described whether the connection point moved or not. If true, then two more cells were consulted, with the four positions given by the binary value of the two cells. Thus each connection point was represented by three cells in the gene string. These points were still valid even if one or both of the elements were no longer in existence in the current model.

The rectangular wing model consisted of 2 spars, 10 ribs, and an upper and lower skin element. The spars were thus split into 10 separate sections each by the ribs. At each split, a connection point was defined. Thus, the model could be represented by a gene string of length L defined by:

$$L = a \times i + b \times j + c \times k + d \times m \qquad (2)$$

where:

    a = skin element cells required (2)

    b = rib element cells required (1)

    c = spar element cells required (1)

    d = connection point cells required (3)

and:

    i = number of skin elements (2)

    j = number of rib elements (10)

   k = number of spar elements (20)

    m = number of connection points (20)

Thus for the model, the gene string is 94 cells long. Even for this relatively simple model with few parameters for optimisation, the number of total possible configurations is 2^{94}, which is a considerable search space.

Flutter Speed (ft/s)	Mass (lbm)	Max Vertical Gust Deflection (ft)
227.70	67.55	4.53

Table 4 Initial Model Performance Data
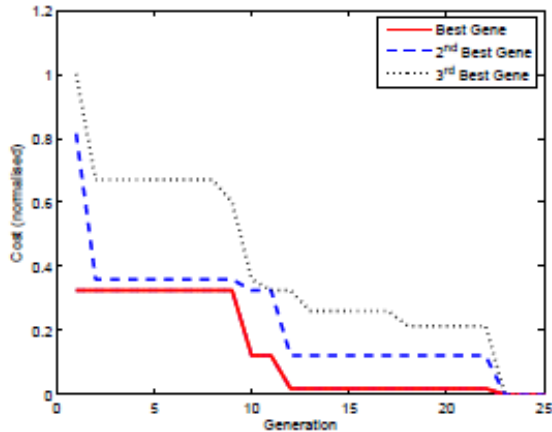
Fig. 5 Typical cost function evolution
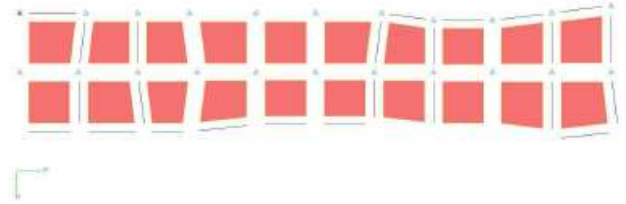

Fig. 6 Optimised Structure for Gene 1

3.4 Discussion

Firstly, the initial model's flutter and gust performance was analysed in order to set a baseline for comparison. The model has the initial performance parameters as listed in table 5.

In figure 4.1, cost is seen to reduce over time from an initial normalised value of 1 to approximately 0.4 by the 8th generation. With the bias set to entirely favour the flutter speed, significant improvements (on average a 213% increase) in the flutter speed are seen even in the low number of generations. Gust deflection also sees improvement with an average 30% reduction. Mass stays fairly consistent throughout the optimisation process. Run 1 (with the full weighting for

Fig. 7 Optimised Structure for Gene 2

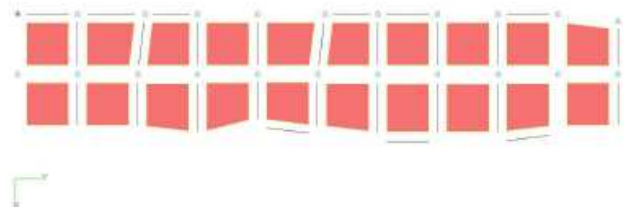|	Gene 1	Gene 2	Gene 3
Cost	0.019	0.1213	0.2146
Flutter Speed (%)	0.44	65.93	54.05
Mass (%)	65.93	99.06	0.20
Gust Deflection (%)	6.34	0.20	14.69

Table 5 Best Genes Result for $W_F = 0$, $W_M = 0.1$ and $W_G = 0.9$
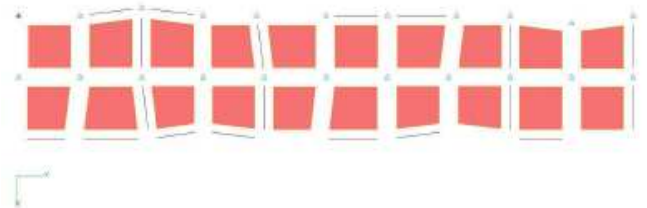
Fig. 8 Optimised Structure for Gene 3

flutter speed) was the only run to see an over-all improvement in flutter speed. In run 2, nor-malised cost again reduces over time, showing the optimisation process works (see figure 4.1). Despite still being heavily weighted towards flut-ter velocity and the cost function converging tem-porarily at approximately 0.4, the average flutter velocity is only 75% of the initial value. Gust de-flection makes a considerable improvement, with the partially optimised on average only 25% of the initial deflection. Again, table 4.3 shows that mass has made no improvement. Run 3, with an even flutter/gust bias for the cost function, dis-plays the same uneven trend towards gust min-imisation as run 2 (see table 4.4). In this run, the cost function also reaches a lower value than the two previous flutter biased runs (figure 4.9). Flutter velocity is again less than the original model, with an average of only 80% of the initial value. Mass remains constant at approximately 99%, and gust deflection shows significant re-duction to 20% of the initial deflection. Run 4 was more heavily biased towards gust deflection, with bias values of [0.225, 0.1, 0.675] for flut-ter, mass and gust criteria respectively. The cost function reached a lower value than the previous 3 runs, with an average below 0.2. The flutter velocity is again lower than the initial value, at 91%. Mass stays constant, and gust deflection achieves a new low of 14% of initial deflection. Finally, in run 5, the outcome of a fully gust-biased optimisation is seen. The run also con-tinues past 8 generations and converges after 22 generations. Flutter velocity is not included in the normalised cost function, and subsequently has no effect on the guidance of the optimisation. The best solution achieved a cost value of 2% of initial value, which is an extreme outcome of the cost function. The average of the 3 genes was a cost value of 0.12. Looking at the corresponding flutter and gust deflection values, flutter velocity is essentially zero for the best gene, and the aver-age is less than 50% of the initial value. Whilst this has no impact on the cost, it is interesting to notice that compared to the opposite end of the bias spectrum which was tested in run 1, the flut-ter speed is detrimentally affected by optimisa-tion biased towards gust deflection. The first run showed improvement in gust response despite not impacting the cost function at all. Finally, the mass has again not played any role in the opti-misation process, staying constant at just below the initial value. Of note is the fact that not all three genes have been constant for the previous generation. Gene 3 continues to improve despite the convergence being declared. As such, results for this test could be improved on what they are already. From these 5 runs, several trends can be observed in the results which can be used to tune the cost function for future optimisation prob-lems. Firstly, the cost function appears to be un-fairly weighted towards the gust response, with even minor weightings showing a distinct ten-dency to optimise the gust parameter over flutter. Only with full bias (sans mass bias component) towards flutter was the outcome of the initial opti-misation favourable to flutter velocity. In all other runs, flutter velocity was negatively impacted in the optimisation process, despite still being heav-ily biased in run 2 and equally biased with gust in run 3. On the converse, all bias settings were ben-eficial to gust response, even when the bias value was zero for gust. This would suggest that ei-ther the gust-focussed biases are Pareto efficient, and the gust cannot be improved drastically fur-ther without negatively impacting flutter velocity, or that the cost function needs revision. Since gust response improved even when flutter speed increased as the focus of run 1, it is more likely to be the second option. Secondly, despite getting a constant 10% weighting in all runs, the mass criteria has little to no impact on the outcome of the tailoring process. This is most likely due to the fact that the only way that the mass criteria can be improved in the current model is by re-moval of spar or rib sections, which most likely has significant impact on the directional stiffness of the wing. This inturn impacts flutter veloc-ity (and to a lesser extent gust response) nega-tively. Even removing a considerable number of elements (figures 4.3, 4.8, 4.11 etc. reduces the overall structural weight by no more than 3% at the maximum. Removing the mass value in this case and giving extra weighting to either flutter or

gust response in future runs would make the optimisation more effective. Finally, the initial generations showed a high rate of improvement, with the cost reducing rapidly to less than half the initial value in only a few generations. This is most likely due to the high number of genes per generation run, allowing for more rapid early improvement, coupled with the low number of purely random genes introduced (3 of 25 per generation).

In run 1, the 3 genes (figures 4.2Ű4.4) can be seen to have a fairly random layout of ribs and spars. Movement of the connection points is mainly arbitrary. The front and rear spar are discontinous, which appears not to impact too greatly on the directional stiffness of the wing. Static strength however is most likely reduced compared to the initial model. One trend that is recognisable is that the inner half of the wingbox contains only a few ribs, compared to the outer section. The number 1 rib and number 6 rib are present in all three models. This however could be entirely random. In run 2, discontinous spars on present on all three models again (figures 4.6, 4.7 and 4.8). The connection points are moved randomly, or at least without discernible pattern. In the first two models, the ribs are more numerous on the outer half of the span, although the third model is grouped clearly in the middle. Runs 3 and 4 again show no real trends in terms of rib or spar placement (see figures 4.10Ű4.12 and 4.14Ű4.16). Run 5 has a slightly more continuous pattern to the spars, with long sections split by several missing spar sections, as opposed to multiple randomly selected short sections. This is most evident in figure 4.18. Overall, there is little evidence in these runs to determine patterns or trends in structural layout as a result of optimisation. However, due to the limited number of generations run, and the high number of variables involved in the structural layout, this is not conclusive proof that there is no positive correlation between spar/rib placement and flutter/gust response. It is quite possible that longer runs would produce noticeable patterns.

Although previous studies have already covered skin laminate orientations in much greater detail, they were added to the optimisation pa-

rameters as an attempt to compare the known effectiveness towards improving aeroelastic response and the unknown effects of the other parameters used. In all the runs, many different combinations of upper and lower skin orientations were encountered. No two models in the same bias group had matching skin orientations. In the first two runs (flutter focussed) the best models from each both had the same skin angles: [+45.,+90.]. The next two runs (3 and 4) were more weighted towards gust minimisation, and the most effective models shared the skin angles: [+45.,.45.], which were only slightly different to the first two runs. Other than this, no real trends emerged as to optimal ply orientation, although the majority of plies in the best models from each run had laminates with the ply orientation spanwise across the wing, as opposed to the initial model with chordwise plies.

4   Conclusions

The optimisation method produced significant improvement in aeroelastic response over a low number of generations, although these improvements were affected strongly by the bias values. In particular, it was found that the cost function favoured improving gust deflection over flutter speed. Whilst a strong correlation between bias at the extremes of the spectrum and better results for either flutter velocity or gust was determined, Mass had very little impact on the outcome.

There was no real pattern recognised between results for various runs and the spar/rib configurations of the models involved. This is not conclusive of the lack of a relationship however as the optimisation test runs failed to converge fully. The high number of variables, coupled with the low number of generations of 4 out of 5 test runs produced a wide range of models, which were not able to be focussed and refined in the generations available.

Finally, despite numerous previous studies linking laminate orientation (and hence directional stiffness) to improved aeroelastic performance, the small sample size meant that these trends could not be accurately identified in the

optimised models.

References

[1] M.M Munk. Propeller containing diagonally disposed fibrous material. US Patent 2,484,308,1111, Oct 1949.

[2] H. Ashley, L. L. Lehman, and J. K. Nathman. The constructive uses of aeroelasticity. In *AIAA International. Annual Meeting and Technical Display*, number 80-0877, 1981.

[3] M.H. Shirk, T.J. Hertz, and T.A. Weisshaar. Aeroelastic tailoring - theory, practice and promise. *Journal of Aircraft*, 23(1):6–18, 1986.

[4] H. Arizono and K. Isogai. Application of genetic algorithm for aeroelastic tailoring of a cranked-arrow wing. *Journal of Aircraft*, 42(2):493–499, 2005.

[5] D.-H Kim, S.-W. Oh, I. Lee, J.-H. Kweon, and J.-H. Choi. Weight optimization of composite flat and curved wings satisfying both flutter and divergence constraints. *Key Engineering Materials*, 334-335:477–480, 2007.

[6] M. Kameyama and H. Fukunaga. Optimum design of composite wings for aeroelastic characteristics using lamination parameters. *Computers & Structures*, 85(3-4):213–224, 2007.

[7] T.A. Weisshaar and D.K. Duke. Induced drag reduction using aeroelastic tailoring with adaptive control surfaces. *Journal of Aircraft*, 43(1):157–164, 2006.

[8] J. Rocha, C. Ramos, and Z. Vale. Process planning using a genetic algorithm approach. In *IEEE International Symposium on Assembly and Task Planning*, Porto, Portugal, 1999.

[9] M.F. Platten, J.R. Wright, K. Worden, G. Dimitriadis, and J.E. Cooper. Non-linear identification in modal space using a genetic algorithm approach for model selection. *International Journal of Applied Mathematics and Mechanics*, 3(1):72–89, 2007.

[10] G.A. Vio and J.E. Cooper. Optimisation of composite wing structures for passive gust alleviation. In *RAeS Aircraft Structural Design Conference*, Liverpool UK, 2008.

[11] J.R. Fuller. Evolution of airplane gust loads design requirements. *Journal of Aircraft*, 32(2):235–246, 1995.

[12] M. Karpel. Design for active flutter suppression and gust alleviation using state-space aeroelastic modelling. *Journal of Aircraft*, 19(3):221–227, 1982.

[13] H. Bohret, B. Krag, and J. Skudridakis. Olga - an open loop gust alleviation system. In *AGARD*, 1984.

[14] F. Abdelmoula. Design of an open-loop gust alleviation control system for airborne gravimetry. *Aerospace Science and Technology*, 3(6):379–389, 1999.

[15] D. Soreide, R.K. Bogue, L.J. Ehernberger, and H. Bagley. Coherent lidar turbulence measurement for gust load alleviation. Technical Memorandum 104318, NASA, 1996.

[16] C.E.S. Cesnik, M. Ortega-Morales, and M.J. Patil. Active aeroelastic tailoring of high aspect ratio composite wings. In 41st *Structures, Structural Dynamics, and Material Conference*, Atlanta, Georgia, 2000.

[17] C.E.S. Cesnik and M. Ortega-Morales. Active aeroelastic tailoring of slender flexible wings. In *International Forum of Aeroelasticity and Structural Dynamics*, Madrid, Spain, 2001.

[18] F. M. Hoblit. *Gust loads on aircraft: concept and applications*. AIAA Educational Series, 1988.

5 Copyright Statement